The Journal of Experimental Biology 202, 3049–3056 (1999)
Printed in Great Britain © The Company of Biologists Limited 1999
JEB2238

PRIMITIVE ORGANIZATION OF CYTOSOLIC Ca^{2+} SIGNALS IN HEPATOCYTES FROM THE LITTLE SKATE *RAJA ERINACEA*

MICHAEL H. NATHANSON[1,2,*], ALLISON F. O'NEILL[1,2] AND ANGELA D. BURGSTAHLER[1,2]

[1]*Mount Desert Island Biological Laboratory, Salsbury Cove, ME 04672, USA* and [2]*Liver Study Unit, Yale University School of Medicine, New Haven, CT 06520, USA*

*Author for correspondence at address 2 (e-mail: michael.nathanson@yale.edu)

Accepted 14 September; published on WWW 28 October 1999

Summary

Cytosolic Ca^{2+} (Ca_i^{2+}) signals begin as polarized, inositol 1,4,5-trisphosphate (InsP3)-mediated Ca_i^{2+} waves in mammalian epithelia, and this signaling pattern directs secretion together with other cell functions. To investigate whether Ca_i^{2+} signaling is similarly organized in elasmobranch epithelia, we examined Ca_i^{2+} signaling patterns and InsP3 receptor (InsP3R) expression in hepatocytes isolated from the little skate, *Raja erinacea*. Ca_i^{2+} signaling was examined by confocal microscopy, InsP3R expression by immunoblot, and the subcellular distribution of InsP3Rs by immunochemistry. ATP induced a rapid increase in Ca_i^{2+} in skate hepatocytes, as it does in mammalian hepatocytes. Unlike in mammalian hepatocytes, however, the Ca_i^{2+} increase in skate hepatocytes began randomly throughout the cell rather than in the apical region. In cells loaded with heparin ATP-induced Ca_i^{2+} signals were inhibited, but de-*N*-sulfated heparin was not inhibitory, suggesting that the increases in Ca_i^{2+} were mediated by InsP3. Immunoblot analysis showed that the type I but not the types II or III InsP3R was expressed in skate liver. Confocal immunofluorescence revealed that the InsP3R was distributed throughout the hepatocyte, rather than concentrated apically as in mammalian epithelia. These findings demonstrate that ATP-induced Ca_i^{2+} signals are mediated by InsP3 in skate hepatocytes, as they are in mammalian hepatocytes. However, in skate hepatocytes Ca_i^{2+} signals begin at loci throughout the cell rather than as an organized apical-to-basal Ca_i^{2+} wave, which is probably because the InsP3R is distributed throughout these cells. This primitive organization of Ca_i^{2+} signaling may in part explain the observation that Ca^{2+}-mediated events such as secretion occur much less efficiently in elasmobranchs than in mammals.

Key words: Cytosolic Ca^{2+}, inositol 1,4,5-trisphosphate, confocal microscopy, elasmobranch, *Raja erinacea*.

Introduction

Cytosolic Ca^{2+} (Ca_i^{2+}) is a second messenger in virtually all types of tissues (Berridge, 1993; Clapham, 1995). In polarized epithelia, Ca_i^{2+} is particularly important for regulating secretory processes, including fluid and electrolyte secretion (Kasai and Augustine, 1990; Ito et al., 1997), exocytosis (Maruyama et al., 1993; Ito et al., 1997), paracellular permeability (Nathanson et al., 1992b) and motility of the subapical cytoskeleton (Nathanson et al., 1992b; Watanabe et al., 1985). In mammalian epithelia, the spatial pattern of Ca_i^{2+} signals is highly organized, and this spatial organization may help direct secretion. For example, apical-to-basal Ca_i^{2+} waves direct fluid and electrolyte secretion by sequential activation of apical and then basal ion channels (Kasai and Augustine, 1990), while localized apical Ca_i^{2+} increases can initiate apical exocytosis (Ito et al., 1997). The polarized organization of Ca_i^{2+} waves in mammalian epithelia probably results from the polarized distribution of the inositol 1,4,5-trisphosphate (InsP3) receptor (InsP3R) in such cells, since epithelial Ca_i^{2+} signals generally are usually mediated by InsP3 (Berridge, 1993), and the InsP3Rs are concentrated in an apical 'trigger zone' in which Ca_i^{2+} waves originate (Nathanson et al., 1994a,b; Yule et al., 1997; Lee et al., 1997). Epithelial secretion appears to be Ca_i^{2+}-mediated in elasmobranchs as well, but occurs much more slowly than in mammals (Nathanson and Mariwalla, 1996). One possible explanation is that the organization of epithelial Ca_i^{2+} signals is more primitive in elasmobranchs, so that Ca_i^{2+} drives secretion less efficiently in these cells. We therefore examined the subcellular organization of Ca_i^{2+} signals and InsP3Rs in polarized preparations of hepatocytes isolated from the little skate *Raja erinacea.*

Materials and methods

Animals and materials

Male skates (*Raja erinacea*, 0.7–1.2 kg) caught by net in

Frenchmen's Bay, ME during the summer of 1998 were used for all experiments. Skates were maintained in large tanks with flowing, 15 °C sea water at Mount Desert Island Biological Laboratory (Salsbury Cove, ME) for up to 4 days prior to use. Adenosine 5′-triphosphate (ATP), low molecular mass heparin, de-*N*-sulfated heparin and poly-L-lysine (molecular mass 150,000–300,000 Da) were obtained from Sigma Chemical Company (St Louis, MO), and rhod-2/AM, rhodamine 123, and fluorescein-conjugated dextran (molecular mass 10,000 Da) were obtained from Molecular Probes (Pitchford, OR). All other chemicals were of the highest quality commercially available.

Preparation of isolated skate hepatocytes

Hepatocytes were isolated by collagenase perfusion as described previously (Nathanson et al., 1995; Nathanson and Mariwalla, 1996). Briefly, each skate was placed on an operating table with running sea water (15 °C) and anesthetized using sodium pentobarbital (0.1 mg kg^{-1}, intravenously via the tail vein). The portal vein was cannulated, then the liver was flushed with heparin (40 000 i.u.), removed and perfused at 15 °C with elasmobranch Ringer solution consisting of NaCl (270 mmol l^{-1}), KCl (4 mmol l^{-1}), $MgCl_2$ (3 mmol l^{-1}), $CaCl_2$ (2.5 mmol l^{-1}), Na_2SO_4 (0.5 mmol l^{-1}), KH_2PO_4 (1 mmol l^{-1}), $NaHCO_3$ (8 mmol l^{-1}), Hepes (5 mmol l^{-1}), glucose (5 mmol l^{-1}) and urea (350 mmol l^{-1}). The liver was perfused for 15 min in a non-recirculating fashion with Ca^{2+}- and Mg^{2+}-free Ringer solution containing heparin (1000 i.u. ml^{-1}), then for 5–10 min in a recirculating fashion in Ringer solution containing collagenase (100 i.u. ml^{-1}). When the perfusion was stopped, the liver was placed in Ringer solution containing deoxyribonuclease II (100 i.u. ml^{-1}), and hepatocytes were manually dispersed with forceps. The isolated hepatocytes were passed twice through a 60 μmol l^{-1} nylon mesh filter, subjected to centrifugation twice at 100 ***g*** and the pellet rinsed, then resuspended at 15 °C in Ringer solution until ready for use. The resulting isolated hepatocytes consisted of both single cells and incompletely digested clusters of 2–20 cells. The cell clusters retain structural and functional polarity (Henson et al., 1995; Miller et al., 1996) and were manually identified and used for these studies.

Cytosolic Ca^{2+} measurements in single cells

Ca_i^{2+} was measured in individual skate hepatocytes using confocal microscopy (Nathanson and Mariwalla, 1996). Cells were prepared as described above, then loaded with rhod-2/AM (4 μmol l^{-1}) for 1–2 h at 15 °C in elasmobranch Ringer solution containing 10 % fetal calf serum. The cells were then plated onto polylysine (1 mg ml^{-1})-coated coverslips and transferred to a chamber on the stage of an Olympus IX-70 inverted microscope, perfused at room temperature (21-23 °C) with buffer and observed using an Olympus Fluoview confocal imaging system. A krypton–argon laser was used to excite the rhod-2 at 568 nm and emission signals above 585 nm were collected. Neither autofluorescence nor other background signals were detectable at the machine settings (i.e. PMT voltage, gain and offset) that were used.

Ca_i^{2+} signals in the hepatocytes were detected using confocal line scanning microscopy (Nathanson and Burgstahler, 1992b; Nathanson and Mariwalla, 1996). With this approach, fluorescence is determined at each point along a single line across the image, rather than at each point across the entire image. This approach permits increased temporal resolution of Ca_i^{2+} signals, with negligible photobleaching and without loss of spatial resolution along the line that is scanned (Nathanson and Burgstahler, 1992a). Cells were observed through a 20× objective lens, with a temporal resolution of 31 ms $pixel^{-1}$ and a spatial resolution of 0.35–0.92 μm $pixel^{-1}$. The change in fluorescence over time in each hepatocyte along the scan line was determined subsequently from the recorded image. Although absolute Ca_i^{2+} concentrations were not estimated because rhod-2 cannot be ratio-imaged (Minta et al., 1989), line scanning measurements were not limited by use of rhod-2 because Ca_i^{2+} signaling patterns (including Ca_i^{2+} wave speeds) are determined independently of Ca_i^{2+} concentration (Nathanson and Burgstahler, 1992a,b). Ca_i^{2+} signaling patterns in single, isolated hepatocytes were observed in response to ATP (100 μmol l^{-1}), either in the presence or absence of extracellular Ca^{2+} (2.5 mmol l^{-1}).

In selected experiments, mitochondria were identified in skate hepatocytes using rhodamine 123 (12.7 μmol l^{-1}). Cells were pre-incubated with the dye for at least 10 min, then observed using confocal microscopy as described previously (Nathanson and Burgstahler, 1992a).

*Cell loading with heparin and de-*N*-sulfated heparin*

In selected experiments, isolated skate hepatocytes were loaded with heparin to block InsP3R-mediated Ca_i^{2+} signaling or with de-*N*-sulfated heparin as a negative control; heparin is a high-affinity competitive antagonist of the InsP3R (Ghosh et al., 1988) while its de-*N*-sulfated analog interacts minimally with this receptor (Tones et al., 1989). Cells were loaded by transient permeabilization in Ca^{2+}-free medium, using a modification of a procedure described previously (Nathanson et al., 1992a). Isolated hepatocytes were incubated at 18 °C for 30 min in an intracellular-like solution containing KCl (120 mmol l^{-1}), glucose (5.6 mmol l^{-1}), EGTA (3 mmol l^{-1}), Hepes (25 mmol l^{-1}) and 5 % fetal calf serum, then heparin (10 mg ml^{-1}) or de-*N*-sulfated heparin (10 mg ml^{-1}) was added together with fluorescein-conjugated dextran (molecular mass 10 000 Da; 0.5–0.75 mg ml^{-1}) as a marker of successful loading. Cells were agitated on ice for 30 min, rinsed and suspended in Ca^{2+}-free elasmobranch Ringer solution, then Ca^{2+} was added to the medium in a stepwise fashion over 15 min. These cells were plated onto glass coverslips and loaded with rhod-2 as described above, then stimulated with ATP (10 μmol l^{-1}) while being examined by confocal video microscopy (Nathanson and Mariwalla, 1996).

Western blot analysis

Immunoblotting of skate liver was performed using separate

antibodies directed against the types I, II and III InsP3R. Liver was probed for the type I InsP3R using rabbit polyclonal antibody T210 directed against the 19 C-terminal amino acids of the mouse type I InsP3R (Takei et al., 1992; Mignery et al., 1989), for the type II receptor using affinity-purified rabbit polyclonal antibody CT2 directed against the C terminus of the rat type II InsP3R (Wojcikiewicz, 1995; Lee et al., 1997), and for the type III receptor using a commercially obtained mouse monoclonal antibody directed against the N-terminal portion of the human type III InsP3R (mAb InsP3R-3; Transduction Laboratories, Lexington, KY) (Lee et al., 1997; Hagar et al., 1998).

Skate liver was homogenized in sample buffer (Laemmli, 1970), and boiled for 5 min. The samples were then electrophoresed through a 6 % SDS/polyacrylamide gel, electrophoretically transferred onto an Immobilon polyvinylidene membrane, and incubated with either the type I, type II or type III InsP3R antibody. Protein extracts from rat cerebellum, rat liver and HeLa cells were used as positive controls for the types I, II and III InsP3R, respectively (Takei et al., 1992; Wojcikiewicz, 1995; Hagar et al., 1998). Immunoreactive bands were incubated with peroxidase conjugates, then detected using an enhanced chemiluminescence kit (Amersham, Arlington Heights, IL).

Confocal immunofluorescence histochemistry

To determine the subcellular distributions of the three InsP3R isoforms, isolated clusters of skate hepatocytes were labeled with the isoform-specific antibodies described above. Specimens were colabeled with rhodamine–phalloidin (Molecular Probes) because this stain identifies the apical pole of hepatocytes (Nathanson et al., 1994a; Fallon et al., 1995).

Immunochemistry was performed on freshly isolated polarized preparations of skate hepatocytes. Tissue was fixed by perfusion with 4 % acetone in 0.12 mol l^{-1} sodium phosphate buffer (pH 7.4), cryopreserved overnight in 15 % sucrose, and frozen in isopentane/liquid nitrogen. After quenching with 50 mmol l^{-1} NH_4Cl and 16 % goat serum in phosphate-buffered saline (PBS) with Triton X-100, the sections were labeled overnight with a 1:10 dilution of antibody T210, a 1:100 dilution of antibody CT2 or a 1:50 dilution of InsP3R-3 antibody, then washed and incubated with FITC-conjugated anti-mouse or anti-rabbit secondary antibody (Sigma), together with rhodamine–conjugated phalloidin (Nathanson et al., 1994a). Negative controls were not incubated with anti-InsP3R antibodies, but were otherwise processed as above. Specimens were examined with the Olympus Fluoview Confocal Microscope described above. To ensure specificity of InsP3R staining, images were obtained using confocal machine settings at which no fluorescence was detectable in negative control samples labeled with secondary antibody alone. Double-labeled specimens were serially excited at 488 nm and observed at >510 nm to detect FITC, then excited at 568 nmol l^{-1} and observed at >585 nm to detect rhodamine. This approach eliminated bleed-through of FITC fluorescence into the rhodamine channel (Nathanson et al., 1994b).

Statistical analysis

For Ca_i^{2+} measurements, comparisons between groups were made using a two-sample *t*-test. There is wide variability of Ca_i^{2+} signals among skate hepatocytes (Nathanson et al., 1995; Nathanson and Mariwalla, 1996); to minimize potential sources of this variability, hepatocytes were only compared to cells isolated from the same liver preparations. Results are expressed as means ± S.E.M, unless stated otherwise.

Results

Organization of subcellular Ca^{2+} signals in isolated skate hepatocytes

The long wavelength Ca^{2+}-sensitive fluorescent dye rhod-2 was used to detect Ca_i^{2+} in isolated skate hepatocytes, since autofluorescence can be significant at lower wavelengths in this cell type (Nathanson and Mariwalla, 1996). However, under certain conditions rhod-2 can preferentially accumulate in mitochondria rather than in cytosol (Hajnóczky et al., 1995). To ensure rhod-2 staining in skate hepatocytes was cytosolic, we therefore compared cells loaded with rhod-2 to those loaded with the mitochondrial dye rhodamine 123 (Fig. 1). Rhod-2 labeling (Fig. 1A,B) was excluded from fat globules that are abundant in this cell type, but was otherwise nearly uniform throughout the cell, as is seen with cytosolic dyes (Nathanson and Burgstahler, 1992a). Rhodamine 123 (Fig. 1C,D) was also excluded from fat globules, but labeled the remainder of cells in a punctate fashion characteristic of the distribution of mitochondria (Nathanson and Burgstahler, 1992a). These findings suggest that rhod-2 accumulates in cytosol rather than mitochondria in this cell type.

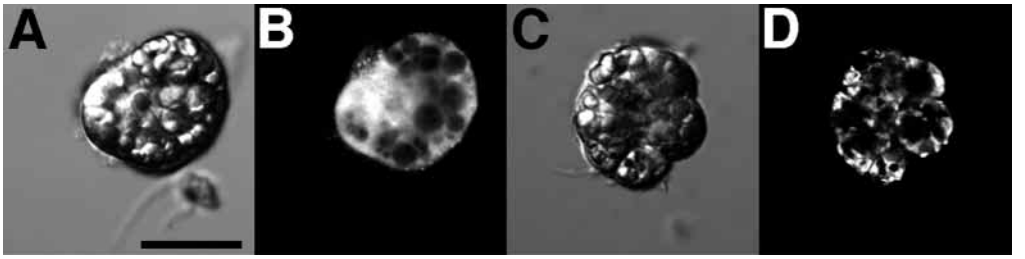

Fig. 1. Rhod-2 labels cytosol rather than mitochondria in isolated skate hepatocytes. (A) Transmission and (B) corresponding confocal fluorescence image of isolated skate hepatocytes loaded with the Ca^{2+} dye rhod-2. (C) Transmission and (D) corresponding confocal fluorescence image of isolated skate hepatocytes loaded with the mitochondrial dye rhodamine 123. In contrast to rhod-2 labeling, rhodamine 123 labeling is distributed in a punctate fashion throughout the cell, characteristic of the distribution of mitochondria. Scale bar, 25 μm.

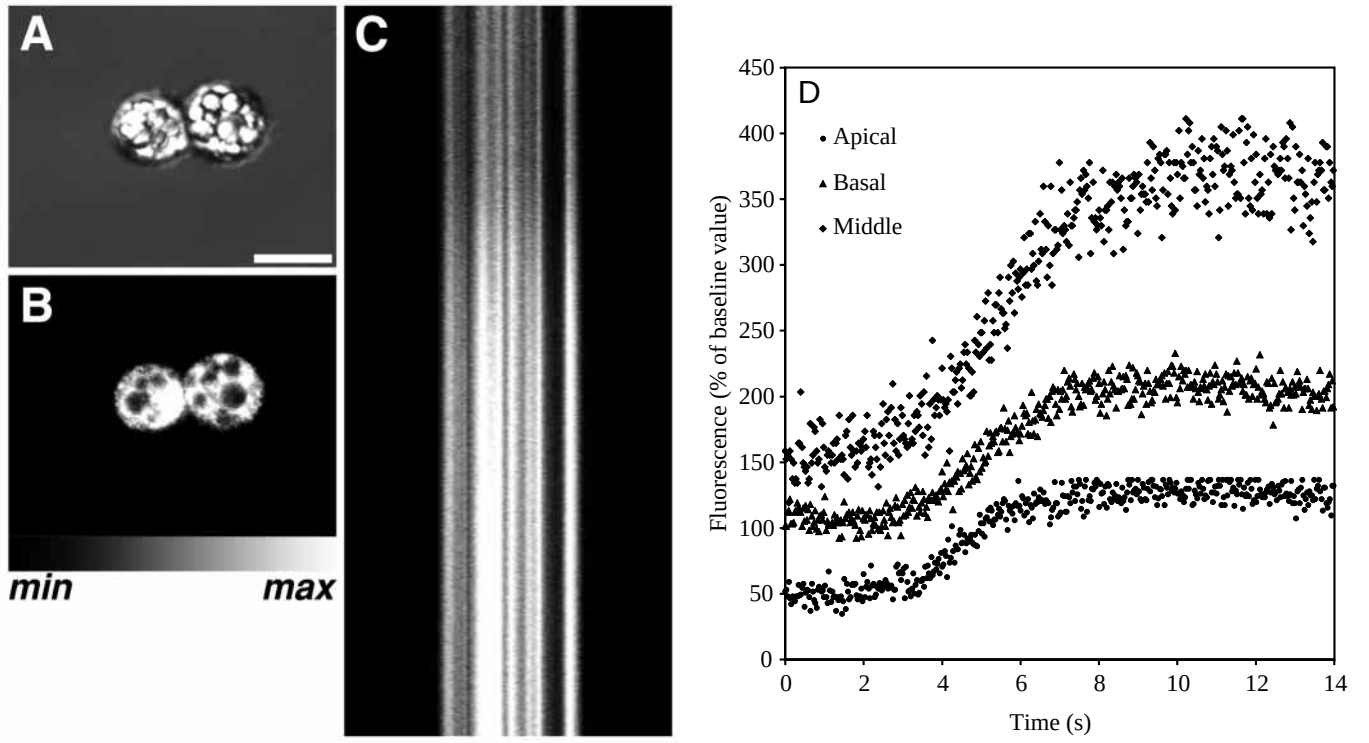

Fig. 2. Subcellular Ca_i^{2+} signaling in isolated skate hepatocytes, detected by confocal line scanning microscopy. (A) Transmission and (B) corresponding confocal fluorescence image of an isolated skate hepatocyte couplet loaded with rhod-2. The intensity of rhod-2 fluorescence in B and C is indicated by the scale below B. Scale bar, 25 μm. (C) Corresponding line scan obtained along the long axis of the couplet in B during stimulation with ATP (100 μmol l^{-1}). Spatial resolution (along the horizontal axis) is the same as in A and B and temporal resolution (along the vertical axis) is 31 ms $pixel^{-1}$ (14 s from top to bottom). (D) Graphical representation of the increase in fluorescence detected in the apical, basal and middle regions of the cell shown in A–C. The increase occurs nearly simultaneously throughout the cell, and the finding is representative of that seen in 15 of 20 cells.

Isolated skate hepatocytes were stimulated with ATP (100 μmol l^{-1}) in order to increase Ca_i^{2+} (Nathanson et al., 1995; Nathanson and Mariwalla, 1996). Ca_i^{2+} signaling was detected in hepatocytes within incompletely digested clusters of cells, since structural and functional polarity is maintained in this type of preparation (Henson et al., 1995; Miller et al., 1996). Ca_i^{2+} signaling was monitored using confocal line scanning microscopy, by orienting the scan line along the apical-to-basal axis of each cell studied (Fig. 2). In most cells (75 %; *N*=15/20), increases in Ca_i^{2+} began at multiple initiation sites rather than as a single transcellular wave (Fig. 2C,D). Specifically, Ca_i^{2+} increases began simultaneously in multiple subcellular regions in 40 % (*N*=8/20) of cells, or else did not progress sequentially from either the apical to the basal or the basal to the apical region of the hepatocyte in 35 % (*N*=7/20) of cells. In the remaining 25 % (*N*=5/20) of hepatocytes, organized apical-to-basal Ca_i^{2+} waves could be identified, but even among these cells there was marked cell-to-cell variation in wave speed (35.4±26.9 μm s^{-1}; mean ± S.E.M). Increases in Ca_i^{2+} began nearly simultaneously at multiple sites throughout the cell in nearly all hepatocytes stimulated with ATP (100 μmol l^{-1}) in Ca^{2+}-free medium as well (95 %; *N*=18/19). Under these conditions, an organized, apical-to-basal Ca_i^{2+} wave was seen in only a single hepatocyte. Similarly, no single initiation site was routinely identified in hepatocytes stimulated with a minimal concentration of ATP (1 μmol l^{-1}). Ca_i^{2+} signals began apically in 31 % (*N*=12/39) of such cells, basolaterally in 43 % (*N*=17/39), and at multiple sites throughout the cell in the remaining 26 % (*N*=10/39). These findings suggest that, in skate hepatocytes, ATP-induced increases in Ca_i^{2+} begin at multiple initiation sites throughout the cell, rather than as a polarized Ca_i^{2+} wave.

ATP-induced Ca^{2+} signals in skate hepatocytes are mediated by InsP3

The role of InsP3 in ATP-induced Ca_i^{2+} signaling was examined by stimulating hepatocytes loaded with either heparin (10 mg ml^{-1}) or de-*N*-sulfated heparin (10 mg ml^{-1}). Cells were loaded during transient permeabilization (Nathanson et al., 1992a). To identify which cells were permeabilized sufficiently to permit loading of low molecular mass heparin (6,000 Da) or its de-*N*-sulfated analog, cells were simultaneously exposed to fluorescein-conjugated dextran (10,000 Da), and only those cells loaded with the dextran were examined (Fig. 3). An increase in rhod-2 fluorescence was seen in only 23 % (*N*=7/31) of heparin-loaded skate hepatocytes stimulated with ATP (10 μmol l^{-1}), and fluorescence increased by only 40±7 % relative to baseline in

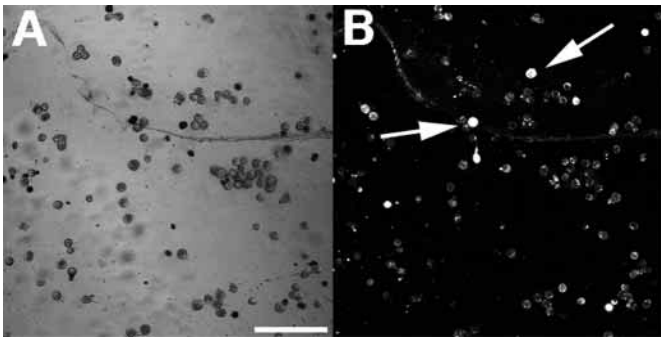

Fig. 3. Transient permeabilization of skate hepatocytes to load macromolecules. (A) Transmission and (B) corresponding confocal fluorescence image of skate hepatocytes loaded with fluorescein-conjugated dextran. Note that only occasional cells are loaded with the dextran (arrows). Scale bar, 100 μm.

those cells. In contrast, ATP increased fluorescence in half (*N*=7/14) of the hepatocytes loaded with de-*N*-sulfated heparin ($P<0.001$ relative to the fraction of heparin-loaded cells that responded, using the normal approximation to the binomial distribution; Afifi and Azen, 1979), and the fluorescence increase in these cells was 68±17 % relative to baseline. For comparison, ATP increased rhod-2 fluorescence in 70 % (*N*=35/50) of hepatocytes not loaded with either heparin or de-*N*-sulfated heparin, and the fluorescence increase among those cells was 76±7 % relative to baseline ($P<0.05$ relative to heparin; $P>0.3$ relative to de-*N*-sulfated heparin). These findings demonstrate that heparin significantly inhibits ATP-induced Ca_i^{2+} signals in skate hepatocytes, whereas de-*N*-sulfated heparin does not. This in turn suggests that these Ca_i^{2+} signals are mediated by InsP3.

Expression and distribution of InsP3R isoforms in skate hepatocytes

Western blotting was performed to determine which isoforms of the InsP3R are expressed in skate liver. Isoform-specific antibodies detected the presence of the type I but not the type II or type III InsP3R (Fig. 4A–C). Immunochemistry was performed to determine the subcellular distribution of the type I InsP3R (Fig. 5) and to confirm lack of expression of the type II and type III isoforms. Hepatocytes were colabeled with rhodamine–phalloidin to label hepatocellular actin, which is distributed along the plasma membrane and is most concentrated in the region of the apical membrane (Henson et al., 1995). Phalloidin staining confirmed that individual hepatocytes within clusters retained structural polarity (Fig. 5A), and helped determine whether InsP3Rs in individual cells were distributed in a polarized fashion. Labeling for the type I InsP3R was distributed heterogeneously throughout each hepatocyte, without a relative increase in staining in either the apical or basolateral region (Fig. 5B,C). No specific InsP3R labeling was detected in cells stained with either the type II or type III InsP3R antibody (not shown), consistent with the results of immunoblotting. Together, these findings demonstrate that skate hepatocytes express the type I but not type II or type III InsP3R, and that the type I InsP3R is distributed throughout the cell.

Discussion

We have examined subcellular Ca_i^{2+} signaling in hepatocytes from the little skate *Raja erinacea*. We examined Ca_i^{2+} signals initiated by ATP, which is the only known Ca_i^{2+} agonist for this tissue (Nathanson et al., 1995; Nathanson and Mariwalla, 1996). Stimulation by ATP increases Ca_i^{2+} through two broad classes of receptors, designated P2X and P2Y (Burnstock, 1996). P2X receptors are ligand-gated Ca^{2+} channels, whereas P2Y receptors are G protein-coupled and increase Ca_i^{2+} via InsP3 (Burnstock, 1996). Previous (Nathanson and Mariwalla, 1996) and current work together suggest that ATP increases Ca_i^{2+} via P2Y receptors in skate hepatocytes, since the increases in Ca_i^{2+} are preserved in Ca^{2+}-free medium and are mediated by InsP3. In addition we found that ATP-induced Ca_i^{2+} signals began nearly simultaneously at random sites throughout each cell. InsP3Rs were distributed nearly uniformly throughout each cell, which is probably why increases in Ca_i^{2+} began in this random fashion. In contrast, hormone-induced increases in Ca_i^{2+} begin as highly organized apical-to-basal Ca_i^{2+} waves in mammalian epithelia (Nathanson et al., 1992c; Kasai and Augustine, 1990; Thorn et al., 1993; Kasai et al., 1993), including rat hepatocytes (Nathanson et al., 1994a). Ca_i^{2+} signaling is mediated by InsP3 in mammalian epithelia (Berridge, 1993; Nathanson, 1994), and this polarized Ca_i^{2+} signaling pattern has been attributed to the fact that the InsP3R is concentrated at the apical pole in such cells (Nathanson et al., 1994a,b; Nathanson, 1994; Yule et al., 1997; Lee et al., 1997). The current findings thus suggest that InsP3-mediated Ca_i^{2+} signaling in epithelia is conserved

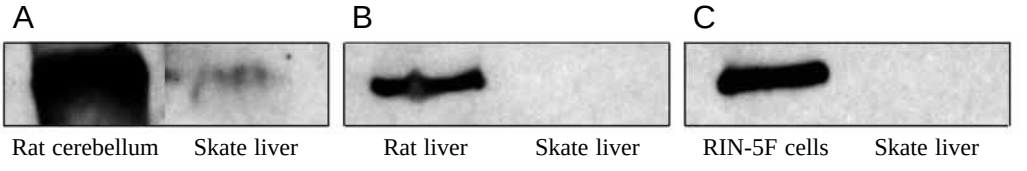

Fig. 4. Skate hepatocytes express the type I but not the type II or type III InsP3 receptor. (A) Western blot analysis using type I-specific InsP3R antibody T210 identifies a single band of the same size in lysates from skate liver and the positive control, rat cerebellum. (B) Western blot analysis using type II-specific InsP3R antibody CT2 identifies a single band in lysate from the positive control rat liver but not in lysate from skate liver. (C) Western blot analysis using a monoclonal type III-specific InsP3R receptor antibody identifies a single band in lysate from the positive control RIN-5F cells but not in lysate from skate liver.

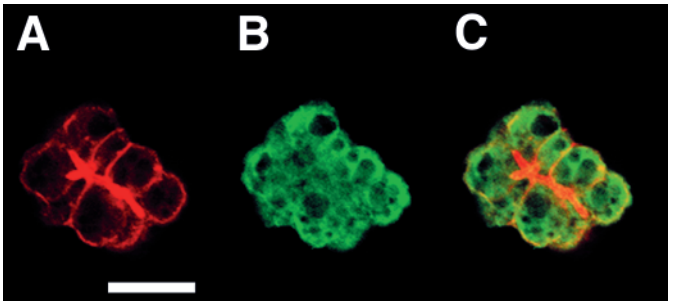

Fig. 5. Subcellular distribution of InsP3 receptors in skate hepatocytes, as determined by confocal immunofluorescence microscopy. (A) Rhodamine–phalloidin labeling of an isolated cluster of skate hepatocytes identifies the plasma membranes of the cells. Labeling is most intense along the apical membranes. (B) Distribution of the type I InsP3R, labeled with antibody T210. No labeling was seen in hepatocytes stained with primary antibody directed against the type II or type III InsP3R, or in cells stained with secondary antibody alone. (C) Superimposed images A and B, demonstrating the nonpolarized distribution of the type I InsP3R in skate hepatocytes. Receptor labeling is diffusely distributed, rather than being concentrated in an apical trigger zone. Scale bar, 50 μm.

from elasmobranchs to mammals, but that the polarized distribution of Ca^{2+} release channels and Ca_i^{2+} signaling patterns seen in mammals evolved after elasmobranchs.

Three isoforms of InsP3R have been described (Maranto, 1994; Sudhof et al., 1991; Furuichi et al., 1989), each of which is an InsP3-gated Ca^{2+} channel (Bezprozvanny et al., 1991; Hagar et al., 1998; Ramos-Franco et al., 1998). For each isoform, the open probability of the Ca^{2+} channel also depends on the Ca_i^{2+} concentration. However, the nature of this Ca_i^{2+} dependence differs, depending on the isoform. The type I InsP3R exhibits a bell-shaped dependence on Ca_i^{2+}, and this characteristic is thought to be responsible for signaling patterns such as Ca_i^{2+} oscillations (Bezprozvanny et al., 1991). This is consistent with the current observation that skate hepatocytes express the type I isoform, since ATP can elicit Ca_i^{2+} oscillations in these cells (Nathanson and Mariwalla, 1996). In contrast to the type I InsP3R, the open probability of both the type II and III receptor increases monotonically as Ca_i^{2+} increases (Hagar et al., 1998; Ramos-Franco et al., 1998). These isoforms thus may be expected to behave as positive feedback Ca^{2+} channels (Hagar et al., 1998). In fact, cells expressing only the type III isoform appear to exhibit all-or-none Ca^{2+} release in response to InsP3 (Hagar et al., 1998). It has therefore been hypothesized that the type III receptor (and thus perhaps the type II receptor) would serve to initiate Ca_i^{2+} signals in cells that express multiple InsP3R isoforms (Hagar et al., 1998). Indeed, in several types of mammalian epithelia the type III isoform is concentrated in the trigger zone from which Ca_i^{2+} waves originate (Nathanson et al., 1994b; Yule et al., 1997; Lee et al., 1997). Thus, the disorganized spatial pattern of Ca_i^{2+} signaling in skate hepatocytes may reflect not only that the InsP3R is distributed in a diffuse rather than a localized fashion in these cells, but also that neither the type II nor type III isoform of the receptor is present to provide an initiation site for the Ca_i^{2+} signal. These findings may also suggest that Ca_i^{2+} signaling via the type I isoform of the InsP3R represents a more primitive or highly conserved mechanism than signaling via either the type II or type III isoform.

What is the physiological role of Ca_i^{2+} signals in skate liver? Ca_i^{2+} modulates secretion in a number of mammalian epithelia (Nathanson, 1994), and ATP-induced Ca_i^{2+} signals are also associated with a threefold increase in bile secretion in skate liver (Nathanson and Mariwalla, 1996). This increase in bile flow is highly transient, however, lasting less than 15 min (Nathanson and Mariwalla, 1996). Furthermore, bile secretion is a much slower process in skates than in mammals. Typical basal rates of bile flow in the isolated perfused skate liver are $<0.1\,\mu l\,g^{-1}\,liver\,min^{-1}$ (Nathanson and Mariwalla, 1996), whereas typical basal bile flow rates in the isolated perfused rat liver are approximately $1–2\,\mu l\,g^{-1}\,liver\,min^{-1}$ (Nathanson et al., 1992a). How do ATP-induced Ca_i^{2+} signals stimulate bile flow in skate liver? Although increases in Ca_i^{2+} activate a range of secretory processes in mammalian epithelia (Nathanson, 1994), several lines of evidence suggest that Ca_i^{2+} may increase bile flow in skate liver simply by inducing contraction of the biliary tree, thereby forcing preformed bile out of the liver. Increases in Ca_i^{2+} cause the subapical network of actin to contract in rat hepatocytes (Watanabe et al., 1985), and skate hepatocytes possess a similar cytoskeletal architecture (Henson et al., 1995). In addition, serial observations of isolated skate hepatocyte clusters loaded with a fluorescent anion suggest that ATP induces contraction of the canalicular lumen, rather than increased accumulation of the anion in the lumen (M. H. Nathanson and A. F. O'Neill, unpublished observation). Additional work will be needed to demonstrate the extent to which polarized signaling mechanisms are required for efficient secretion, but the primitive organization of Ca_i^{2+} signaling in *Raja erinacea* may provide a useful model for further study of this question.

We thank Pietro DeCamilli for providing InsP3R-1 antibody T210, Richard Wojcikiewicz for providing InsP3R-2 antibody CT2, and David Seward for assistance with hepatocyte isolations. This work was supported by an Established Investigator Grant from the American Heart Association, a Pilot and Feasibility Grant from the Cystic Fibrosis Foundation, NIH Award DK45710, an REU Award from the NSF, the Center for Membrane Toxicity Studies (NIH P30 ES03828) and the Yale Liver Center (NIH P30 DK34989).

References

Afifi, A. A. and Azen, S. P. (1979). *Statistical Analysis: A Computer Oriented Approach*. New York: Academic Press.

Berridge, M. J. (1993). Inositol trisphosphate and calcium signalling. *Nature* **361**, 315–325.

Bezprozvanny, I., Watras, J. and Ehrlich, B. E. (1991). Bell-shaped calcium-response curves of Ins(1,4,5)P_3- and calcium-gated channels from endoplasmic reticulum of cerebellum. *Nature* **351**, 751–754.

Burnstock, G. (1996). P2 purinoceptors: historical perspective and classification. In *P2 Purinoceptors: Localization, Function and Transduction Mechanisms* (ed. D. J. Chadwick and J. A. Goode), pp. 1–34. New York: John Wiley and Sons.

Clapham, D. E. (1995). Calcium signaling. *Cell* **80**, 259–268.

Fallon, M. B., Gorelick, F. S., Anderson, J. M., Mennone, A., Saluja, A. and Steer, M. L. (1995). Effect of cerulein hyperstimulation on the paracellular barrier of rat exocrine pancreas. *Gastroenterology* **108**, 1863–1872.

Furuichi, T., Yoshikawa, S., Miyawaki, A., Wada, K., Maeda, N. and Mikoshiba, K. (1989). Primary structure and functional expression of the inositol 1,4,5-trisphosphate-binding protein P400. *Nature* **342**, 32–38.

Ghosh, T. K., Eis, P. S., Mullaney, J. M., Ebert, C. L. and Gill, D. L. (1988). Competitive, reversible and potent antagonism of inositol 1,4,5-trisphosphate-activated calcium release by heparin. *J. Biol. Chem.* **263**, 11075–11079.

Hagar, R. E., Burgstahler, A. D., Nathanson, M. H. and Ehrlich, B. E. (1998). Type III InsP3 receptor channel stays open in the presence of increased calcium. *Nature* **396**, 81–84.

Hajnóczky, G., Robb-Gaspers, L. D., Seitz, M. B. and Thomas, A. P. (1995). Decoding of cytosolic calcium oscillations in the mitochondria. *Cell* **82**, 415–424.

Henson, J. H., Capuano, S., Nesbitt, D., Hager, D. N., Nundy, S., Miller, D. S., Ballatori, N. and Boyer, J. L. (1995). Cytoskeletal organization in clusters of isolated polarized skate hepatocytes: structural and functional evidence for microtubule-dependent transcytosis. *J. Exp. Zool.* **271**, 273–284.

Ito, K., Miyashita, Y. and Kasai, H. (1997). Micromolar and submicromolar Ca^{2+} spikes regulating distinct cellular functions in pancreatic acinar cells. *EMBO J.* **16**, 242–251.

Kasai, H., Li, Y. X. and Miyashita, Y. (1993). Subcellular distribution of Ca^{2+} release channels underlying Ca^{2+} waves and oscillations in exocrine pancreas. *Cell* **74**, 669–677.

Kasai, H. and Augustine, G. J. (1990). Cytosolic Ca^{2+} gradients triggering unidirectional fluid secretion from exocrine pancreas. *Nature* **348**, 735–738.

Laemmli, U. K. (1970). Cleavage of structural proteins during the assembly of the head of bacteriophage T_4. *Nature* **227**, 680–685.

Lee, M. G., Xu, X., Zeng, W. Z., Diaz, J., Wojcikiewicz, R. J. H., Kuo, T. H., Wuytack, F., Racymaekers, L. and Muallem, S. (1997). Polarized expression of Ca^{2+} channels in pancreatic and salivary gland cells – Correlation with initiation and propagation of $[Ca^{2+}]_i$ waves. *J. Biol. Chem.* **272**, 15765–15770.

Maranto, A. R. (1994). Primary structure, ligand binding and localization of the human type 3 inositol 1,4,5-trisphosphate receptor expressed in intestinal epithelium. *J. Biol. Chem.* **269**, 1222–1230.

Maruyama, Y., Inooka, G., Li, Y. X., Miyashita, Y. and Kasai, H. (1993). Agonist-induced localized Ca^{2+} spikes directly triggering exocytotic secretion in exocrine pancreas. *EMBO J.* **12**, 3017–3022.

Mignery, G. A., Sudhof, T. C., Takei, K. and De Camilli, P. (1989). Putative receptor for inositol 1,4,5-trisphosphate similar to ryanodine receptor. *Nature* **342**, 192–195.

Miller, D. S., Fricker, G., Schramm, U., Henson, J. H., Hager, D. N., Nundy, S., Ballatori, N. and Boyer, J. L. (1996). Active microtubule-dependent secretion of a fluorescent bile salt derivative in skate hepatocyte clusters. *Am. J. Physiol. Gastrointest. Liver Physiol.* **270**, G887–G896.

Minta, A., Kao, J. P. Y. and Tsien, R. Y. (1989). Fluorescent indicators for cytosolic calcium based on rhodamine and fluorescein chromophores. *J. Biol. Chem.* **264**, 8171–8178.

Nathanson, M. H., Gautam, A., Bruck, R., Isales, C. M. and Boyer, J. L. (1992a). Effects of Ca^{2+} agonists on cytosolic Ca^{2+} in isolated hepatocytes and on bile secretion in the isolated perfused rat liver. *Hepatology* **15**, 107–116.

Nathanson, M. H., Gautam, A., Ng, O. C., Bruck, R. and Boyer, J. L. (1992b). Hormonal regulation of paracellular permeability in isolated rat hepatocyte couplets. *Am. J. Physiol. Gastrointest. Liver Physiol.* **262**, G1079–G1086.

Nathanson, M. H., Padfield, P. J., O'Sullivan, A. J., Burgstahler, A. D. and Jamieson, J. D. (1992c). Mechanism of Ca^{2+} wave propagation in pancreatic acinar cells. *J. Biol. Chem.* **267**, 18118–18121.

Nathanson, M. H. (1994). Cellular and subcellular calcium signaling in gastrointestinal epithelium. *Gastroenterology* **106**, 1349–1364.

Nathanson, M. H., Burgstahler, A. D. and Fallon, M. B. (1994a). Multi-step mechanism of polarized Ca^{2+} wave patterns in hepatocytes. *Am. J. Physiol. Gastrointest. Liver Physiol.* **267**, G338–G349.

Nathanson, M. H., Fallon, M. B., Padfield, P. J. and Maranto, A. R. (1994b). Localization of the type 3 inositol 1,4,5-trisphosphate receptor in the Ca^{2+} wave trigger zone of pancreatic acinar cells. *J. Biol. Chem.* **269**, 4693–4696.

Nathanson, M. H., Mariwalla, K., Ballatori, N. and Boyer, J. L. (1995). Effects of Hg^{2+} on cytosolic Ca^{2+} in isolated skate hepatocytes. *Cell Calcium* **18**, 429–439.

Nathanson, M. H. and Burgstahler, A. D. (1992a). Subcellular distribution of cytosolic Ca^{2+} in isolated rat hepatocyte couplets: Evaluation using confocal microscopy. *Cell Calcium* **13**, 89–98.

Nathanson, M. H. and Burgstahler, A. D. (1992b). Coordination of hormone-induced calcium signals in isolated rat hepatocyte couplets: Demonstration with confocal microscopy. *Mol. Biol. Cell* **3**, 113–121.

Nathanson, M. H. and Mariwalla, K. (1996). Characterization and function of ATP receptors on hepatocytes from the little skate *Raja erinacea*. *Am. J. Physiol. Regul. Integr. Comp. Physiol.* **270**, R561–R570.

Ramos-Franco, J., Fill, M. and Mignery, G. A. (1998). Isoform-specific function of single inositol 1,4,5-trisphosphate receptor channels. *Biophys. J.* **75**, 834–839.

Sudhof, T. C., Newton, C. L., Archer, B. T., Ushkaryov, Y. A. and Mignery, G. A. (1991). Structure of a novel $InsP_3$ receptor. *EMBO J.* **10**, 3199–3206.

Takei, K., Stukenbrok, H., Metcalf, A., Mignery, G. A., Sudhof, T. C., Volpe, P. and De Camilli, P. (1992). Ca^{2+} stores in Purkinje neurons: endoplasmic reticulum subcompartments demonstrated by the heterogeneous distribution of the $InsP_3$ receptor, Ca^{2+}-ATPase and calsequestrin. *J. Neurosci.* **12**, 489–505.

Thorn, P., Lawrie, A. M., Smith, P. M., Gallacher, D. V. and Petersen, O. H. (1993). Local and global cytosolic Ca^{2+} oscillations in exocrine cells evoked by agonists and inositol trisphosphate. *Cell* **74**, 661–668.

Tones, M. A., Bootman, M. D., Higgins, B. F., Lane, D. A., Pay, G. F. and Lindahl, U. (1989). The effect of heparin on the inositol

1,4,5-trisphosphate receptor in rat liver microsomes. *FEBS Lett.* **252**, 105–108.

Watanabe, S., Smith, C. R. and Phillips, M. J. (1985). Coordination of the contractile activity of bile canaliculi: Evidence from calcium microinjection of triplet hepatocytes. *Lab. Invest.* **53**, 275–279.

Wojcikiewicz, R. J. H. (1995). Type I, II and III inositol 1,4,5-trisphosphate receptors are unequally susceptible to down-regulation and are expressed in markedly different proportions in different cell types. *J. Biol. Chem.* **270**, 11678–11683.

Yule, D. I., Ernst, S. A., Ohnishi, H. and Wojcikiewicz, R. J. H. (1997). Evidence that zymogen granules are not a physiologically relevant calcium pool – Defining the distribution of inositol 1,4,5-trisphosphate receptors in pancreatic acinar cells. *J. Biol. Chem.* **272**, 9093–9098.